Proceedings, Symposium on Intelligent Systems and Applications SIA2003
Iaşi, Romania, September 19-20, 2003

Editors: Horia-Nicolai Teodorescu, Constantin Gaindric and Emil Sofron
ISBN 973-97737-2-9

Hardware Adaptive System for Movement Artifact Removing – Component of a Virtual Reality System

Dan-Marius Dobrea*, Horia-Nicolai Teodorescu*

*Technical University "Gh. Asachi", Iasi, Faculty of Electronics and Telecommunications

Abstract: The aim of this paper is to present a hardware implementation of an adaptive artifact removing technique, used in a Virtual Reality system. Even if, conceptually, the topology is well known, the hardware implementation of a large part of the system brings several advantages - particularly related to our application but not limited to - that will be shown in the paper. A short comparison between an adaptive method and a classical filter is also presented.

1 Introduction

Mainly because the computational power of the processors significantly increased in the last decade, the adaptive methods (more computational demanding than standard filtering techniques) spread in many fields of science and engineering applications like: medicine and biomedical, physics, aviation, home appliances etc. In biomedical applications, adaptive filtering technique has been shown to be useful in a large class of problems. Starting with the removing of the 50 Hz power line interference, continuing with arrhythmia detection [1], suppression of stimulus artifacts from the evoked potential recordings [2], [3], and ending with detection of the P-waves from the ECG signal [4], these are only few of the possible applications.

From a number of reasons the artifact signals are difficult to be removed from the received signals. First, because the amplitude of the artifacts is a number of times larger than the signal; second, the artifacts overlap – in time and frequency domain – the signal and, third, the artifacts manifest a large variability in frequency and amplitude over the time. From these reasons the classical filtering techniques get poor results and, in many applications, they cannot eliminate the artifacts.

In this paper we will present the implementation of an adaptive system and its results. In essence, mainly because a large part of the adaptive system is hardware implemented the overall performance increased comparing with the software solution implementation. Here, the adaptive system is used to remove a specific type of artifacts from one component of a virtual reality system, employed in user fatigue state identification. The virtual reality system is created from several independent components, which acquire a number of biological signals without any physical contact with the body, and a software processing unit. The presented hardware system is used to remove baseline wander artifacts from the respiratory signal acquired by the Virtual Reality system.

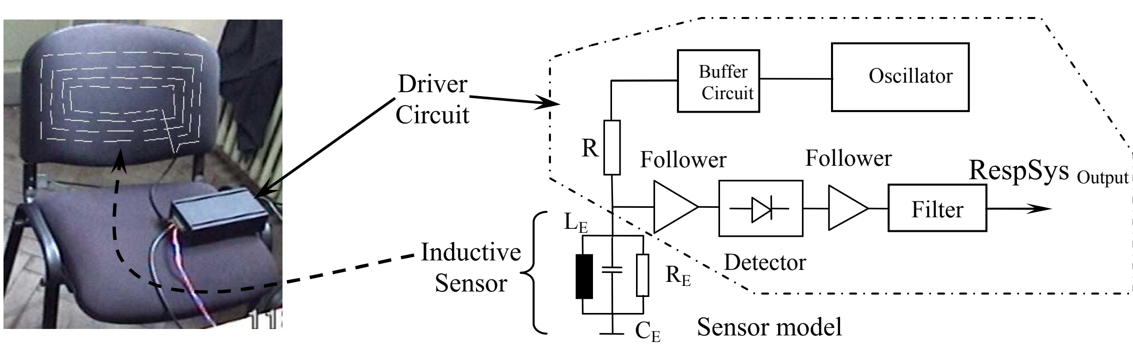

Figure 1 - The respiratory acquisition system and the driver circuit

2 Respiration System Acquisition

The respiratory signal was acquired using the reography (impedancemetry) method [5]. The system's component used to obtain respiratory signal consists in a chair with one sensor [6], [7] embedded in the back support, with no direct contact with the body, **figure 1**. The sensor consists in a coil and its work principle is as following: an element generating an external electromagnetic field changes its impedance due to the properties of the objects in its close vicinity. In our case the change is due to the variation of the equivalent reactive impedance, viewed at the port of the measuring device and given by the chest movements (respiration, small involuntary and voluntary movements). The main idea is to determine the respiratory movements, based on the change of impedance that these movements produce in the sensor. Inherently, the respiratory signal also includes another components such as those derived from the tremor movements, the blood flow induced movements and the heart movements. But, these components are of small values and they do not significantly disturb the acquired respiratory signal. The user's hand and body movements generate the main artifacts that appear and disturb the respiratory signal.

The respiratory signal acquisition was performed with the setup sketched in **figure 1**, consisting in a sensing element placed on the back support of a chair and a circuit that drives the sensing element and process the signal from the sensor. Details of the working mode for the driving circuit are presented in [8]. At the output of the driving circuit **RespSys $_{\mathbf{Output}}$** we get the respiratory signal, contaminated with the movement artifacts.

3 The artifacts

Until now, we used in our research different methods [9] in order to reduce or cancel the movement artifacts from the acquired respiratory signals. The movement artifacts can be classified in two subclasses (from the point of view of artifacts life time versus respiratory signal periods): fast movements (like hand movements) and slow movements (like slowly changes of the body position).

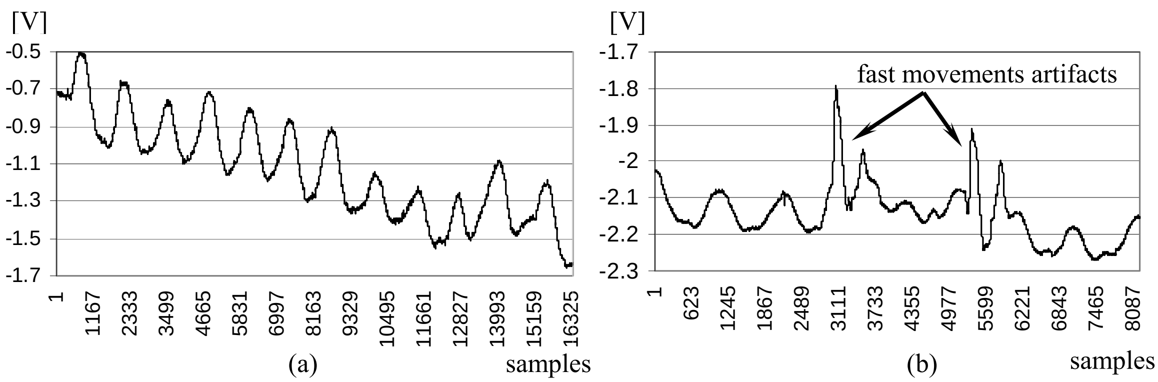

Figure 2 - (a) Baseline wander artifact – determined by a slow movement; (b) Fast movement artifacts

The simultaneously removing of the both type of artifacts (see **figure 2),** without any distortion of the respiratory signal, is almost impossible. In a previously paper [9] we presented a method to deal with the fast movement artifacts. In this paper we will address only the problem of artifacts removing for the case of baseline wander artifacts.

The baseline wander artifact is composed of one DC component - generated by the distance between the subject body torso position and the back chair support (where the sensor is embedded) -, and from another slow time variable component, given by the torso movements. Moreover, the DC component is directly related with the trunk shape variability, user position on the chair and, also, with the chair position (the sensor position), linked with the objects from the close vicinity.

To have a deeper understanding of the respiratory signal's characteristics and its variability (signal contaminated with the baseline wander artifacts) we used the time-frequency analysis as a preliminary step. The ability of the time-frequency analysis to highlight the characteristics of the nonstationary signals and its computationally efficiency (in our case, it incorporates the short time fast Fourier transform) motivate our choice. The time-frequency technique, used in the signal analysis, was the spectrogram, which estimates the power spectral density on sliding windowed segments; in this mode the method accounts the nonstationarity of the respiratory signal. For the analysis done in **figure 3** it was used a Hamming window.

The respiratory signal has a fundamental frequency in the range starting with 0.1 Hz up to 0.3 Hz, for the adult subjects, with a bandwidth in the range 0.05 Hz … 3 Hz [5]. The respiratory signal's fundamental is characterized in **figure 3** by a horizontal band, with the mean frequency at 0.176 Hz. The second order harmonic – a parallel band above the fundamental component – situated around 0.356 Hz indicates that the respiratory signal's oscillation is not a sinusoidal one.

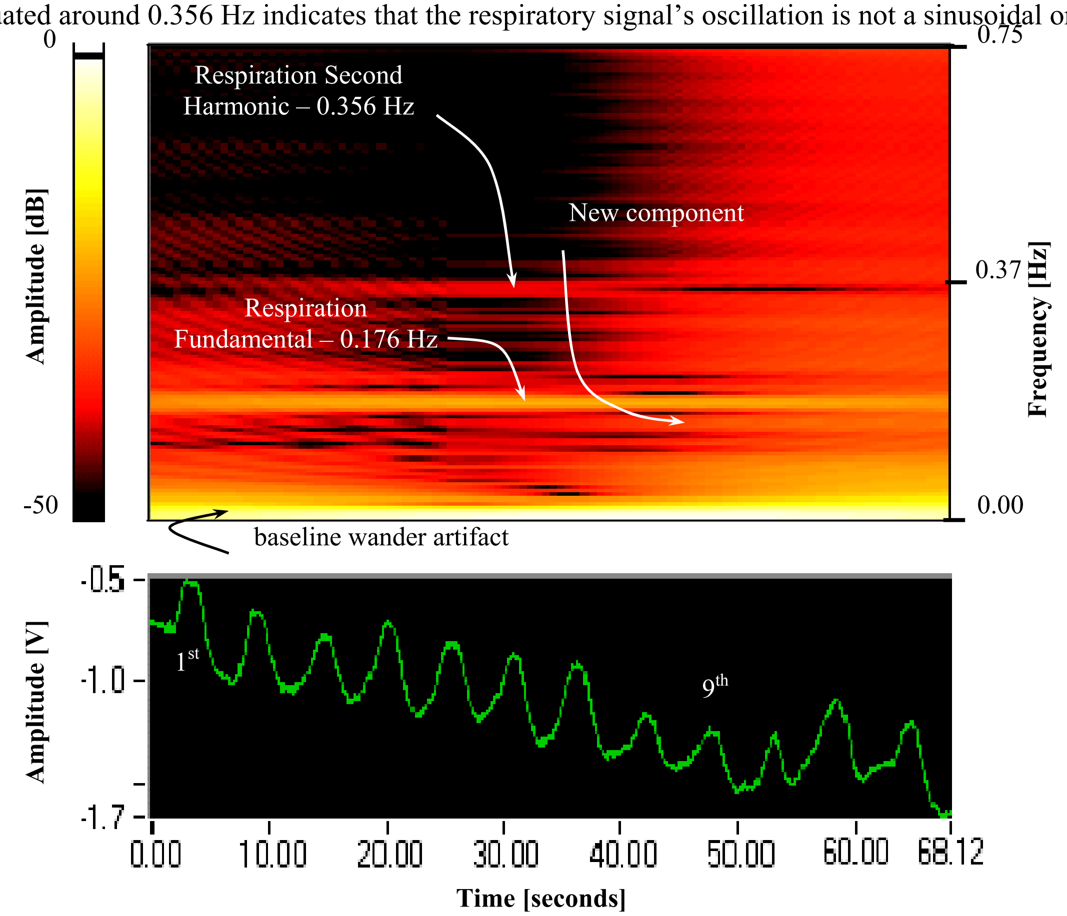

Figure 3 - The top plot shows the spectrogram of a respiratory signal recorded when the user change to trunk position. The bottom plot shows the respiratory signal.

Starting with the 9th period of the respiratory signal or a bit prior of it – when, in the time domain, we can observe a tendency change – we also remark some frequency change in the amplitude's components from the spectrogram. In the upper part of the same image (**figure 3),** we can notice that even the main frequency component is constant, the second order harmonic fades and another component of a lower frequency increases in amplitude. Simultaneously, at the higher frequencies the spectrum starts to become more reach. In the same time, the bandwidth at the lower frequencies increases. It can be seen that both components of the signal, the respiratory and movement artifact, start to increase their bands and overlap.

4 Hardware System for Artifact Removing

The main idea of the adaptive filtering method, used in this research, was presented for the first time in [10]. The adaptive filter has two inputs (**figure 4**). At the primary input we have the signal s_1, contaminated with an additive noise n_1. If at the reference input we have the noise n_2, correlated with n_1, then the error signal will be:

$$\varepsilon = (s_1 + n_1) - y_{adapt} \quad (1)$$

$$\begin{aligned}\varepsilon^2 &= (s_1 + n_1)^2 - 2y_{adapt}(s_1 + n_1) + y_{adapt}^2 = \\ &= (n_1 - y_{adapt})^2 + s_1^2 + 2s_1 n_1 - 2y_{adapt} s_1\end{aligned} \quad (2)$$

Because the signal s_1 and the additive noise n_1 are uncorrelated, the mean-squared error (MSE) is:

$$E[\varepsilon^2] = E[(n_1 - y_{adapt})^2] + E[s_1^2] \quad (3)$$

Minimizing the (3), it result a filter error $\varepsilon \cong s_1$ that is the best least squares estimate of the signal s_1. In our case the s_1 is the respiratory signal and the baseline wander artifact gives the noise, n_1. In order to cancel this slow movement artifact, at the reference input of the adaptive filter a simple constant value (such as 1) is necessary.

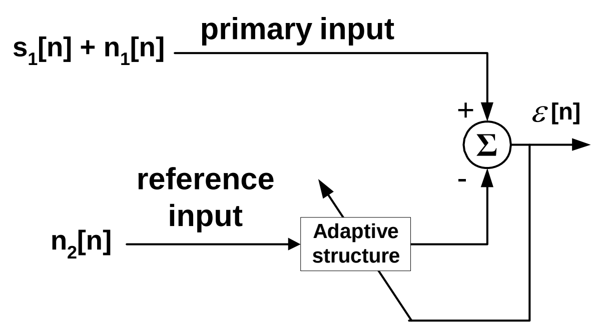

Figure 4 - The adaptive structure used to cancel the slow movement artifacts

In the first implementation of the system, presented in **figure 4**, the circuit topology is like the one shown in **figure 5**. The adaptive structure is a FIR filter with two weights trained with the Least-Mean Squares (LMS) algorithm; it minimizes the MSE between the primary and the reference inputs. The relation used to adapt both weights is:

$$w[n+1] = w[n] + 2 \cdot \eta \cdot \varepsilon[n] \cdot x[n] \quad (4)$$

In the relation (4), $\mathbf{w}[\mathbf{n}] = [w_1, w_2]^T$ is the filter weight vector at the moment $\mathbf{n}$ and $\mathbf{x}[\mathbf{n}] = [x_1, x_2]^T$ is the reference input sample vector, at the same time moment $\mathbf{n}$.

The adaptive filter has a “zero” at the low frequency components and, consequently, it creates a notch with a bandwidth [1] of:

$$\frac{\eta}{\pi} \cdot f_s \quad (5)$$

where f_s is the input signal sampling rate. As we see from (5) the value of the step size controls the cut off filter frequency.

The main disadvantage of this topology consists in the large number of time series lost because of the superior or inferior limitation, given by the dynamic input range of the AT-MIO-16E-10 digital acquisition board (DAQ).

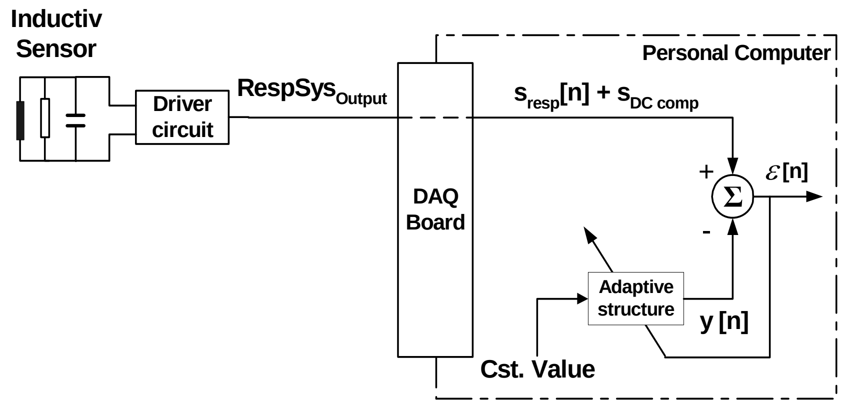

Figure 5 - The implemented structure of the adaptive system

In the design faze of the respiratory acquisition system we imposed two main requirements for it:

- the ability to obtain an accurate respiratory signal – information provided by the A.C. component – and
- the possibility to acquire, in the same time, the distance between the trunk of the subject using the system and the back chair support – information .

The last condition is one necessary for the Virtual Reality system to obtain as much as possible information related with the user subject states. It is known that the body movements are often related with nervosity, lack of attention, motor fatigue and agitation, confusion etc.; hence, it is important to acquire the body movements too. Due to the second goal, the D.C. component cannot be removed before the DAQ board. This leads to the change in solution from the classical one in **figure 5** to the one in **figure 6**.

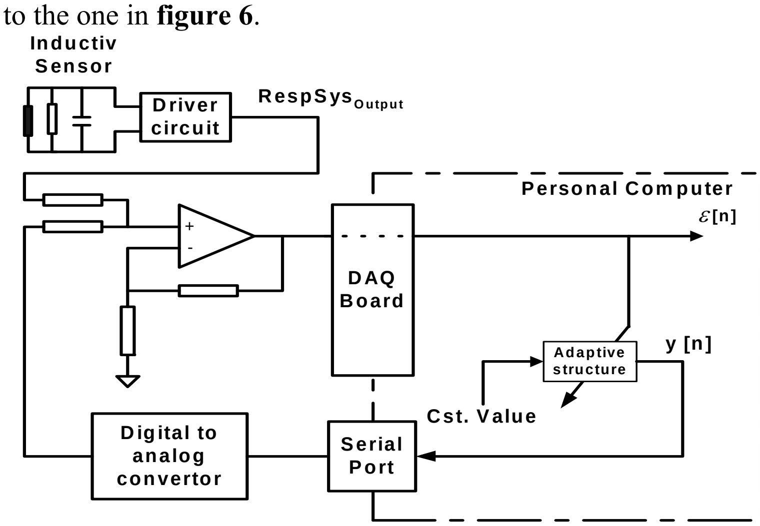

Figure 6 - The second implementation of the adaptive system

The baseline wander signal for our system is in the range of around –4V up to 4V; after the filtering stage of the driver circuit, at the output **RespSys** $_{\textbf{Output}}$, the respiratory signal has a dynamic range, from peek to peek, starting with 4mV and going up to 20-25 mV. In this condition, for our 12 bits DAQ board it can be easily observed that the lower limit of the respiratory range signal is very close to minimum resolution of the DAQ board (for a maximum input dynamic range of -5 … +5V this is 2.44 mV). To have the resulting respiratory signal accurate and independent of user chair position or respiratory chest movement, the signal must be amplified.

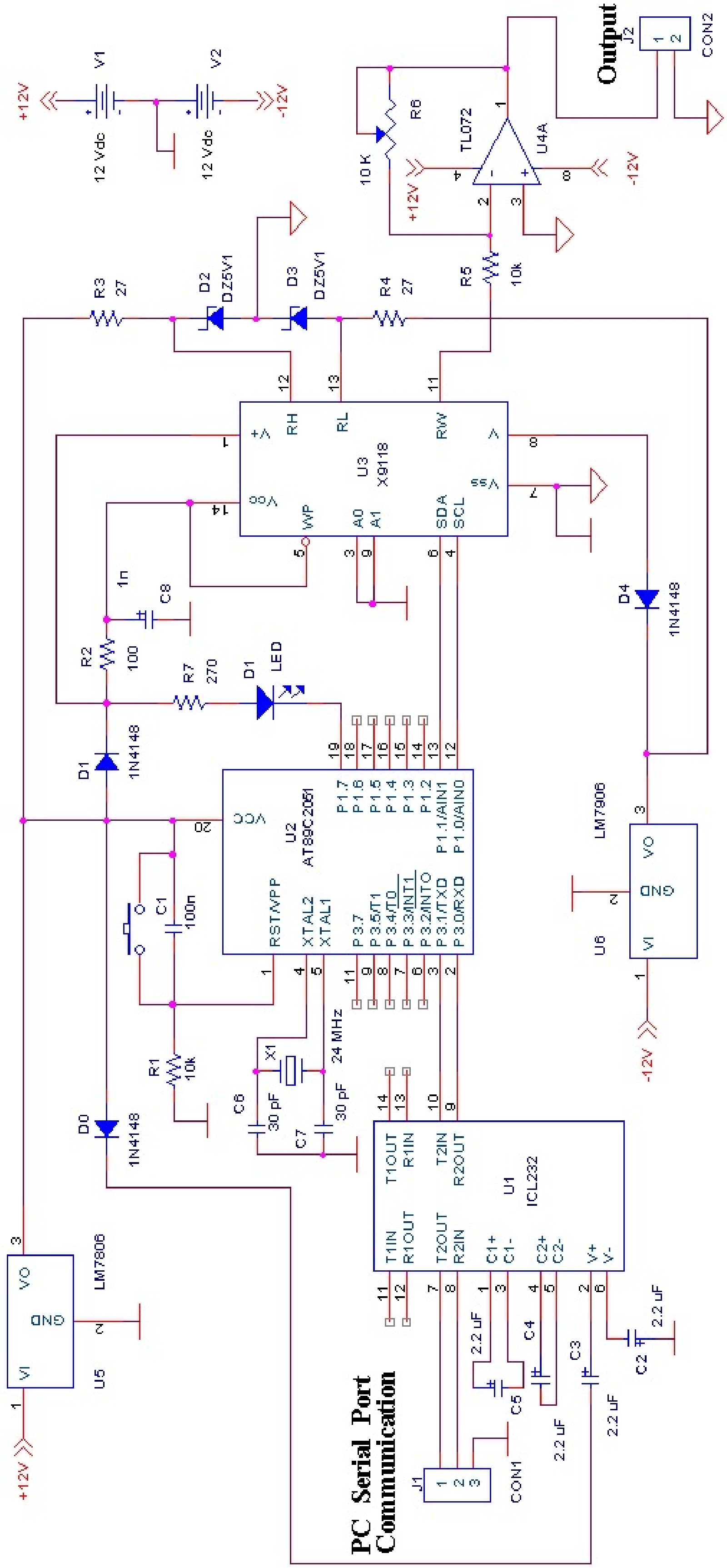

Figure 7 - The digital to analog conversion block

In the worst condition, with a DC component close to 4V and a respiratory signal of 4mV, the DAQ board cannot manage the signal anymore. Thus, if we set a gain of 2 to the DAQ board, we are constrained to have an input in the range of –2.5 … 2.5V in order to obtain, inside the DAQ board, a dynamic range of –5 … +5V. In this situation, the input signal is outside the input dynamic range and, in conclusion, the acquisition is compromised.

Another solution, like that of having two different signal paths for DC component and for the respiratory signal, provides at least two main disadvantages:

- first, as it was seen previously, it is very difficult to choose the two cut frequencies for the analog filters used to discriminate between the signals, mainly because of the dynamics of the signals' spectral components and,
- second, in a such a situation we must use another input differential channel.

Thus, the only reasonable solution is to remove, in an adaptive mode, the DC component before the acquisition. In the second implementation of the adaptive system we propose the following solution sketched in the **figure 6**.

This solution solves the both problems. First, the baseline wander signal is removed in an adaptive mode, before the acquisition to be done with the DAQ board; second, we also have now the equivalent value of the DC component obtained at the output, $y[n]$, of the adaptive filter.

The schematics of the "Digital to analog converter" block is presented in the **figure 7**. The digital controlled potential, applied on the external adder circuit, is controlled by the software adaptive structure through the computer serial line. The $y[n]$ output, on the range of –10V … +10V (**figure** 6), converted to a numeric value between 0 and 1023 is send through the serial port to a microcontroller system build around the AT89C2051 circuit, U2 (**figure 7**). After decoding the serial data the microcontroller commands the digitally controlled potentiometer embedded in U3, X9118 XDCP, through an I2C bus. At the wiper terminal of the potentiometer, RW – pin 11 U3, we will get a potential proportional with the numeric value send through the RS232 serial port interface.

The inverting operational amplifier is mainly used to invert the potential value, in order to obey the schematics block from **figure 4** and to subtract the output of the adaptive circuit from the incoming signal. The U1 circuit is used only to interface the microcontroller with the outside world (the personal computer).

5 Results

In the following we present the results related to the respiratory sequence on which we previously did the time-frequency analysis. To have a clear idea of the adaptive system's performance, a standard filtering technique was used on the same respiratory wave. The filter was a standard high-pass FIR with the pass band frequency at 0.09 Hz (this value was chosen accordingly with **figure 3**, in order to get only the respiratory signal) and a stop band frequency at 0.05 Hz, with a –50 dB attenuation. The output wave of the FIR filter is presented in **figure 8(a);** in the same figure (c) we can see the adaptive filtering result. For the FIR filter the transitory response was removed from the presentation.

From the graphical results presented above it seems that the FIR filter gets a better result in baseline wander artifact removing but, if we get a close look we will also observe that the quality of the respiratory signal obtained by an adaptive procedure is superior. Also, we have to note that the signal given by the FIR filter produces some distortion on the 11^{th} period of the respiratory signal. This respiration period has almost the same amplitude like 9^{th} and 10^{th} wave period. From the original wave (**figure 8**) it can be easily seen that this is not the case. If we ignore the time sifting resulted using the FIR filter we can notice the same result in **figure 9**.

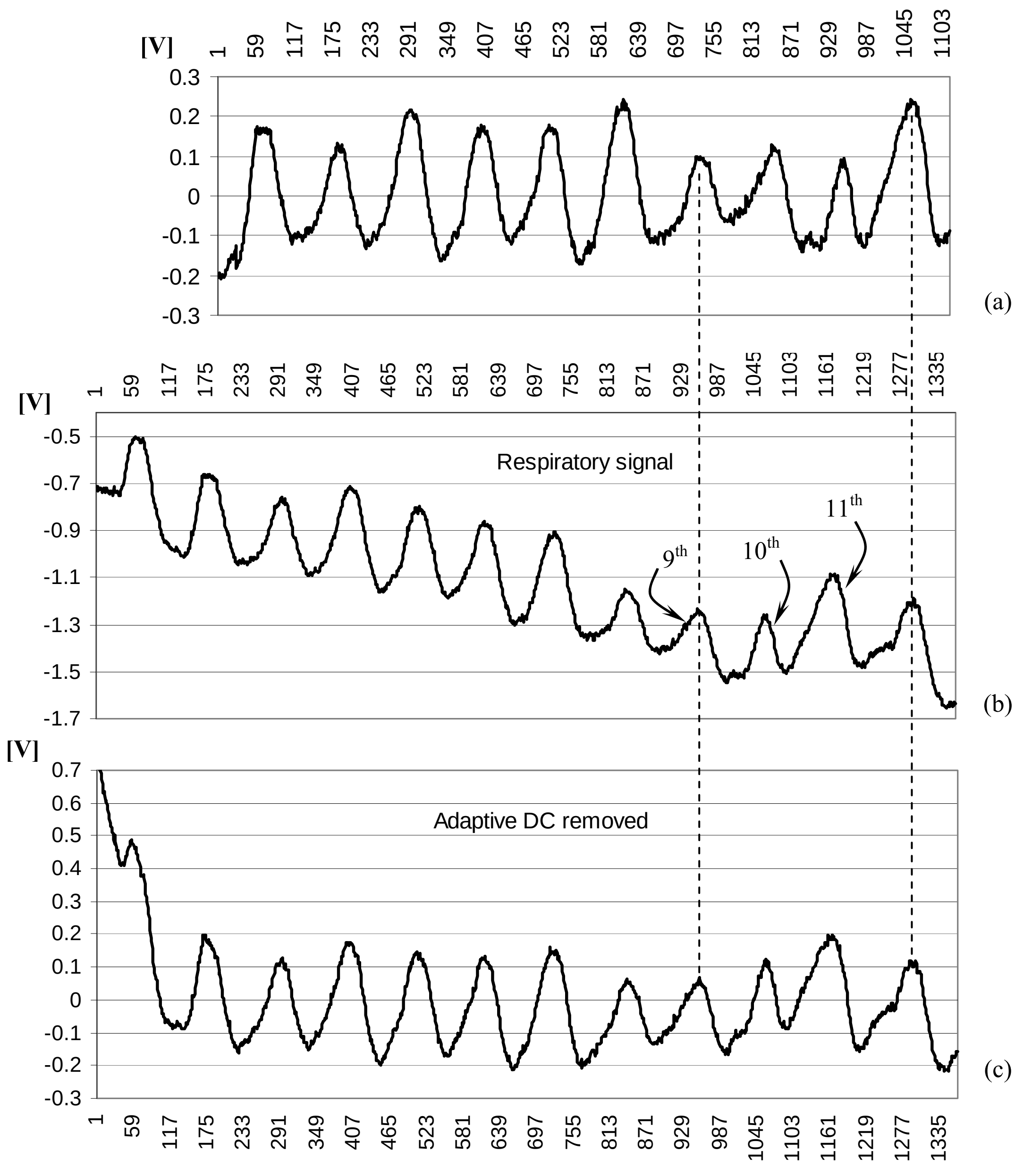

Figure 8 - (a) Resulting respiratory signal using a standard filtering technique (b) The respiratory signal affected by artifact (c) Resulting respiratory signal produced by the adaptive method

The superiority of the results in the case of adaptive filtering method can easily be seen. The 11th respiratory period is qualitatively proportional to the previous respiration period. This is helpfully mainly because we further use the accurate respiratory wave for some parameter's extraction. With these parameters, a classification system will discriminate the fatigue state of the investigated subject.

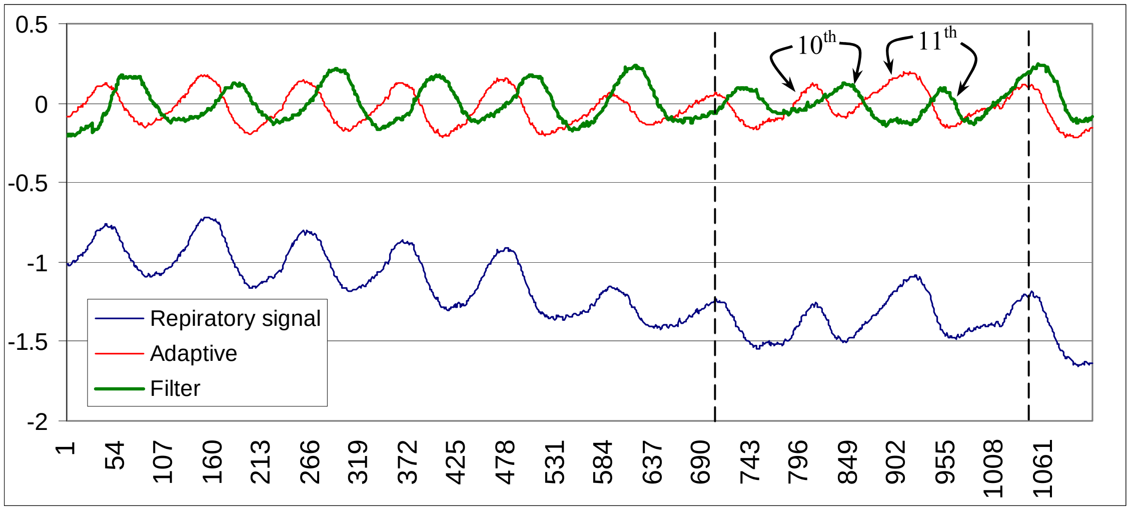

Figure 9 - The respiratory signal affected by artifacts an the two results of the artifacts removing techniques

6 Conclusions

Even if the adaptive method used in this research is a very classical one, superior results can be obtained by a proper implementation.

Both objectives imposed in the design of the respiratory acquisition system were accomplished. Thus, we have an acquisition system able to:

- achieve an accurate respiratory signal moreover,
- use to acquire the distance between the trunk of the subject and the back chair support.

Finally, if we add at this system another software and hardware component for removing the fast movements [9], we get a complete independent system capable to record an accurate, artifact free respiratory signal. Further, this global system could be integrated into a more complex system used to assess the physiological user's state.

References

[1]. N. V. THAKOR, YI-SHENG YHU: *Application of Adapt Filter to ECG Anaysis: Noise Cancellation and Arrhythmia Detection*, IEEE Transaction on Biomedical Engineering, vol. 38, no. 8, pp. 785-794, 1991

[2]. V. PARSA, P. A. PARKER, R. N. SCOTT: *Adaptive Stimulus Artifact Reduction in Noncortical Somatosensory Evoked Potential Studies*, IEEE Transactions on Biomedical Engineering, vol. 45, no. 2, pp. 165-179, 1998

[3]. M. KNAFLITZ, R. MERLETTI: *Suppresion of stimulation artifacts from myoelectric-evoked potential recordings*, IEEE Transactions on Biomedical Engineering, vol. 35, no. 9, pp. 758-763, 1988

[4]. Y. ZHU, N. V. THAKOR, *P-wave detection by adaptive cancelation of the QRS-T complex*, Proccedings of the 8th IEEE Annual Conferince of Biomedical Engineering Society, pp. 329-331, 1986

[5]. H. N. TEODORESCU, D. M. DOBREA: *A system to monitor the respiration and movements without contact with the body*, Proceedings of the European Conference on Intelligent Technologies, ECIT'2000 International Conference, Romania, Iasi, ISBN 973-95156-1-4, 2000

[6]. H. N. TEODORESCU: *Position and movement resonant sensor*, Patent No. 5986549, United States, Publication date: 1999, Oct. 14

[7]. H. N. TEODORESCU, D. M. DOBREA, E. Forte, M. Wentland-Forte: *A High Sensitivity Sensor for Proximity Measurements and Its Use in Virtual Reality Applications*, Proceedings of the European Conference on Intelligent Technologies, ECIT'2000 International Conference, Romania, Iasi, ISBN 973-95156-1-4, 2000

[8]. D. M. DOBREA: *A New Type of Non-Contact 3D Multimodal Interface to Track and Acquire Hand Position and Tremor Signal*, ECIT'2002, European Conference on Intelligent Technologies 2002, July 20-22, Iasi, Romania, ISBN 973-8075-20-3, 2002

[9]. D. M. DOBREA, H. N. TEODORESCU, M. C. SERBAN: *Method to remove respiratory artefacts from a system used to assess the bio-psychic state of a person*, 3rd Symposium on Biomedical Engineering and Medical Physics 2002, 27 August - 1 September, 2002, Patras, Greece

[10]. B. WINDROW, J. R. GLOVER, J. M. MCCOOL: *Adaptive noise cancelling: principles and applications*, Proceedings IEEE, vol. 63, pp. 1692-1716, 1975